ACS OMEGA

Article

Cite This: ACS Omega 2019, 4, 8222−8230

http://pubs.acs.org/journal/acsodf

An Efficient Synthesis of Deoxyrhapontigenin-3-*O*-*β*-D-glucuronide, a Brain-Targeted Derivative of Dietary Resveratrol, and Its Precursor 4′-*O*-Me-Resveratrol

Ângelo de Fátima,*[,†,‡] Maite Docampo-Palacios,[†] Anislay Alvarez-Hernandez,[†] Giulio M. Pasinetti,[§] and Richard A. Dixon*[,†]

[†]BioDiscovery Institute and Department of Biological Sciences, University of North Texas, 1155 Union Circle #311428, Denton, Texas 76203-5017, United States

[‡]Department of Chemistry, Universidade Federal de Minas Gerais, Avenida Presidente Antônio Carlos 6627, Campus Pampulha, Belo Horizonte, Minas Gerais 31270-901, Brazil

[§]Department of Neurology, Icahn School of Medicine at Mount Sinai, One Gustave L. Levy Place, P.O. Box 1230, New York, New York 10029, United States

Supporting Information

ABSTRACT: Bioactive dietary polyphenols have health benefits against a variety of disorders, but some benefits of polyphenols may be not directly related to them but rather to their metabolites. Recently, we have identified the brain-available phenol glucuronide metabolite deoxyrhapontigenin-3-*O*-*β*-D-glucuronide (**5**) in perfused rat brains following subacute treatment with the stilbene resveratrol (**1**). However, the role of such a metabolite in the neuroprotective activity of resveratrol (**1**) is not understood, in part due to the noncommercial availability of **5** for performing biological evaluation in animal models of Alzheimer's disease or other neurological disorders. Here, we describe a concise chemical synthesis of deoxyrhapontigenin-3-*O*-*β*-D-glucuronide (**5**) and its precursor 4-*O*-Me-resveratrol (**2**), accomplished in four and six steps with 74 and 21% overall yields, respectively, starting from commercially available 3,5-dihydroxybenzaldehyde. Pivotal reactions employed in the synthesis include the palladium-catalyzed C−C coupling between 3,5-di-*tert*-butyldiphenylsilyloxystyrene and *p*-iodoanisole in the presence of tributylamine and the acid-catalyzed glucuronidation between the trichloroacetimidate-activated glucuronic acid and 4-*O*-Me-resveratrol.

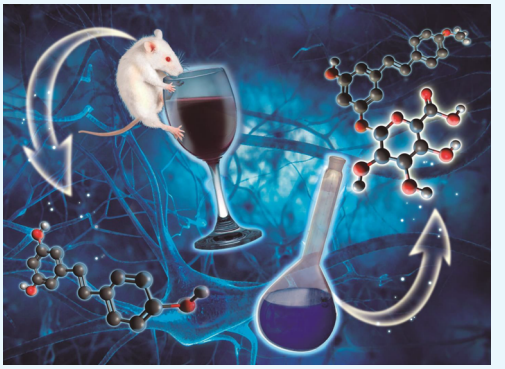

1. INTRODUCTION

Bioactive dietary polyphenols are receiving increasing interest due to their reported health benefits against a variety of disorders[1−7] arising from intestinal absorption, metabolism, and subsequent interactions with target tissues.[8−12] Additionally, some polyphenol metabolites from dietary sources might have more profound biological activities than their precursors.[10,13−16]

Resveratrol (**1**; Figure 1), a polyphenol naturally produced by several plants, is widely reported to be beneficial for human health as an anticancer,[17−19] antidiabetic,[20−22] anti-obesity,[20,23,24] anti-oxidant,[25−28] anti-inflammatory,[29−31] and anti-Alzheimer's disease (AD)[32−35] agent, among others. However, some of these beneficial properties may be not directly related to this polyphenol but rather be a result of its phase II metabolism. For instance, the resveratrol metabolites **2** and **3** (Figure 1) were shown to inhibit the growth of human adenocarcinoma (Caco-2) cells by 80 and 86%, respectively, whereas resveratrol (**1**) at the same concentration impaired the growth by 52%.[36] Patients with colorectal cancer and receiving oral resveratrol (0.5 to 1.0 g/day for 8 days) have high levels of metabolites **2**−**4** (Figure 1) in the colorectum,[37] and metabolite **4** inhibited colon cancer cell proliferation and led to an accumulation of cells in the S phase.[38] Remarkably, the mixture of such metabolites induced a synergistic effect.[38] Furthermore, resveratrol metabolites **3** and **4** (Figure 1) induced similar delipidating effects to resveratrol in maturing pre-adipocytes, and both glucuronide metabolites **2** and **3** showed a depleting effect, although lower than that of resveratrol, in mature adipocytes.[39] These findings suggest that both resveratrol and resveratrol metabolites are involved, to greater or lesser extents, in the anti-obesity effects of these polyphenols,[39] and the literature shows that the activity of resveratrol and/or resveratrol metabolites depends on their distribution and concentration in different tissues and the species used for in vivo studies.[9,40−42]

Flavonoids have been known for some time to impact brain function,[43] and our laboratory and others have shown that

Received: March 20, 2019
Accepted: April 18, 2019
Published: May 7, 2019

DOI: 10.1021/acsomega.9b00722
ACS Omega 2019, 4, 8222−8230

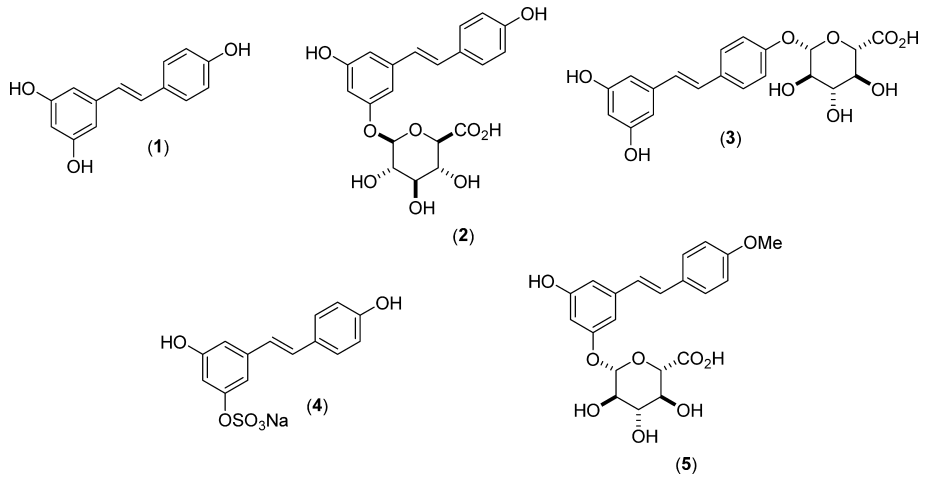

Figure 1. Chemical structures of resveratrol (**1**) and its metabolites resveratrol 3-*O*-*β*-D-glucuronide (**2**), resveratrol 4′-*O*-*β*-D-glucuronide (**3**), resveratrol 3-sulfate (sodium salt) (**4**), and deoxyrhapontigenin-3-*O*-*β*-D-glucuronide (**5**).

grape seed extracts (GSE) and red wine are able to modulate AD phenotypes by modulating multiple disease-modifying modalities via both *β*-amyloid-dependent and *β*-amyloid-independent mechanisms.[44−51] By assessing the accumulation of polyphenols in the brains of rats treated with oral dosage of Cabernet Sauvignon red wine and testing the identified brain-targeted polyphenols for potential beneficial AD disease-modifying activities, we identified quercetin-3-*O*-*β*-D-glucuronide as a novel anti-Alzheimer agent.[16] Our results showed that quercetin-3-*O*-*β*-D-glucuronide may simultaneously modulate multiple independent AD disease-modifying mechanisms and, as such, may contribute to the benefits of dietary supplementation with red wines in AD models.[16] We have also identified resveratrol 3-*O*-*β*-D-glucuronide (**2**) and deoxyrhapontigenin-3-*O*-*β*-D-glucuronide (**5**; Figure 1) in perfused rat brains following subacute treatment with resveratrol (**1**) (300 mg/kg/day for 10 days) (unpublished data). The presence of such metabolites in the rat brain suggests that they can penetrate the blood−brain barrier (BBB) and may thereby play an important role in the anti-AD effect of resveratrol (**1**). It is therefore important to determine if and how these metabolites (**2** and **5**) are involved in the modulation of AD by resveratrol (**1**). However, only the resveratrol 3-*O*-*β*-D-glucuronide (**2**) is commercially available, and there is no chemical synthetic approach described for obtaining deoxyrhapontigenin-3-*O*-*β*-D-glucuronide (**5**). To the best of our knowledge, there is only one microbial synthesis of deoxyrhapontigenin-3-*O*-*β*-D-glucuronide (**5**) described using *Streptomyces* sp. M52104.[52]

Here, we report the first chemical synthesis of deoxyrhapontigenin-3-*O*-*β*-D-glucuronide (**5**) and the synthesis of its precursor 4′-*O*-Me-resveratrol (**2**). The 4′-*O*-Me-resveratrol (**2**) and deoxyrhapontigenin-3-*O*-*β*-D-glucuronide (**5**) were synthesized in four and six steps with 74 and 21% overall yields, respectively.

2. MATERIALS AND METHODS

2.1. General Information. High-performance liquid chromatography (HPLC)-grade solvents were purchased from Fisher Scientific. Chemicals and solvents were of reagent grade and obtained from commercial sources without further purification. All reactions were monitored by thin-layer chromatography (TLC) on aluminum-backed precoated silica gel 60 F254 plates (Sigma, St. Louis, MO), and compounds were detected using $KMnO_4$ (0.5 g) dissolved in 1 N NaOH (100 mL) or H_2SO_4 (5% in water). Column chromatographic purification was performed using 230−400 mesh silica gel, unless otherwise noted. The proton and carbon nuclear magnetic resonance (^{1}H-NMR and ^{13}C-NMR, respectively) spectra were recorded using a Varian-INOVA 500 NMR spectrometer (Varian, CA, USA) at 500 and 125 MHz, respectively. For the NMD analysis, the synthesized substances were dissolved in a specific deuterated solvent [CD_3OD (99.6% atom D; Sigma, St. Louis, MO); acetone-d_6 (99.9% atom D; Sigma, St. Louis, MO); $CDCl_3$ (99.8% atom D; Acros Organics, Morris Plains, NJ)] and then transferred to a 5 mm Shigemi tube (Wilmad Glass, Vineland, NJ). Preparative high-performance liquid chromatography (HPLC) was performed on an Agilent HP1200 HPLC, monitoring at 280 nm. The HPLC with ChemStation software version B.02.01.SRI was equipped with a G1322A degasser, G1311A quaternary pump, G1367B autosampler, G1316A thermostatic column compartment, and G1315C diode array detector. A Phenomenx Luna 10 *μ*m C18(2) 250 × 21.2 mm column was used for preparative HPLC on the Agilent HPLC system. The column was eluted with an isocratic mixture of acetonitrile and water with formic acid (0.1%) (28:72, v/v), and the flow rate was set at 8 mL/min. The detection of newly synthesized metabolites was achieved using a hybrid triple quadrupole/ion trap mass spectrometer QTRAP 5500 from AB Sciex. Each compound was injected individually and directly into the mass spectrometer at a flow rate of 7 *μ*L/min using electrospray ionization. Full and product ion scan modes were utilized to assess precursor ion mass and MS/MS spectrum, respectively. LC−MS/MS data were recorded and processed using Analyst 1.7 software (AB Sciex). Melting points were measured in open capillary tubes on an Electrothermal IA9000 Series apparatus and are uncorrected.

2.2. Synthesis of 4′-*O*-Me-Resveratrol (11). *2.2.1. 3,5-Dihydroxystyrene (7).* 3,5-Dihydroxystyrene (7) was prepared according to the literature procedure.[53] Sodium hydride (NaH) (320 mg, 8.0 mmol) was dissolved in 6 mL of anhydrous DMSO, and the mixture was stirred under a nitrogen atmosphere for 1 h at 70 °C. The mixture was then cooled in an ice bath, and a solution of $CH_3P(C_6H_5)Br$ (2.85 g, 8.0 mmol) in anhydrous DMSO (5 mL) was added dropwise under vigorous stirring. The mixture was then stirred

DOI: 10.1021/acsomega.9b00722
ACS Omega 2019, 4, 8222−8230

Table 1. ^{1}H-NMR (500 MHz) and ^{13}C-NMR (125 MHz), in Acetone-d_6, of 4′-*O*-Me-Resveratrol (11)[a]

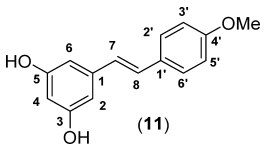

	^{1}H-NMR (δ ppm, J Hz)		^{13}C-NMR (δ ppm)	
atom #	(500 MHz)	lit.[b] (500 MHz)	(125 MHz)	lit.[b] (125 MHz)
1			140.7	140.5
2	6.55, d, J = 2.2	6.54, d, J = 3.0	105.7	105.8
3			159.6	159.2
4	6.28, t, J = 2.2	6.31, t, J = 2.4	102.8	102.8
5			159.6	159.2
6	6.55, d, J = 2.2	6.54, d, J = 3.0	105.7	105.8
7	6.95, d, J = 15.9	6.82, d, J = 16.0	127.5	127.4
8	7.05, d, J = 15.9	6.96, d, J = 16.0	128.8	128.8
1′			131.0	130.7
2′	7.52, d, J = 8.4	7.41, d, J = 8.4	128.6	128.5
3′	6.94, d, J = 8.4	6.88, s	114.9	114.8
4′			160.4	160.1
5′	6.94, d, J = 8.4	6.88, s	114.9	114.8
6′	7.52, d, J = 8.4	7.41, d, J = 8.4	128.8	128.5
OCH_3	3.81, s	3.80, s	55.6	55.8
OH	8.20, br s	7.94, br s		

[a]Reagents and reaction conditions: (a) (i) 1.1 equiv of 2,3,4-tri-*O*-acetyl-α-D-glucuronic acid methyl ester, tricholoroacetamidate, 0.25 equiv of TMSOTf, DCM, 4 Å molecular sieves, 0 °C, 3 h (30%) or (ii) 1.2 equiv of 2,3,4-tri-*O*-acetyl-α-D-glucuronic acid methyl ester, tricholoroacetamidate, 0.70 equiv of BF_3·Et_2O, DCM, 4 Å molecular sieves, 0 °C, 5 h (35%); (b) MeONa/MeOH (5.4 M), NaOH (1.0 M), THF/MeOH (4:1, v/v), 0 °C, 3.5 h (80%). [b]Ref 52.

at room temperature for 10 min, and a solution of 3,5-dihydroxybenzaldehyde (274 mg, 2.0 mmol) in anhydrous DMSO (7 mL) was added dropwise under vigorous stirring and a nitrogen atmosphere for 1 h. The reaction was quenched by addition of 60 mL of diethyl ether and 100 g of ice. The organic phase was separated, and the aqueous phase extracted with diethyl ether (3 × 40 mL). The combined organic phase was dried over anhydrous $MgSO_4$ and filtered, and the solvent was evaporated under vacuum. The residue was subjected to silica gel column chromatography, eluting with hexane/diethyl ether (1:3) to give 3,5-dihydroxystyrene (**7**) as a colorless oil (248 mg, 91%). ^{1}H-NMR (500 MHz, DMSO-d_6): δ 9.22 (s, 2H, 2× OH), 6.53 (dd, J = 10.8, 17.6 Hz, 1H, H2), 6.30 (2× s, 2H, H4 and H8), 6.15 (s, 1H, H6), 5.62 (dd, J = 1.0, 17.6 Hz, 1H, H_{trans}-1a), 5.15 (dd, J = 1.0, 10.8 Hz, 1H, H_{cis}-1b). ^{13}C-NMR (125 MHz, DMSO-d_6): δ 158.5, 138.9, 137.2, 113.2, 104.3, 102.4.

*2.2.2. 3,5-Di-tert-butyldiphenylsilyloxystyrene (**8**).* Imidazole (953 mg, 14.0 mmol) was added to a solution of 3,5-dihydroxystyrene (**7**) (238 mg, 1.75 mmol) in dimethylformamide (2.6 mL), and the mixture was stirred under a nitrogen atmosphere for 15 min at room temperature. The silyl chloride (1.82 mL, 7.0 mmol) was added, and the light yellow solution was stirred for 18 h. The mixture was dissolved in diethyl ether (50 mL), and water (100 mL) was added. The organic phase was separated, and the aqueous phase was extracted with diethyl ether (3 × 50 mL). The combined organic phase was washed with brine (2 × 50 mL) and dried over anhydrous $MgSO_4$, and the solvent was evaporated under vacuum. The residue was subjected to silica gel column chromatography, eluting with hexane/ethyl acetate (15:1) to give 3,5-di-*tert*-butyldiphenylsilyloxystyrene (**8**) as a colorless oil (1.02 g, 95%). ^{1}H-NMR (500 MHz, $CDCl_3$): δ 7.60−7.30 (m, 20H, Ph-H), 6.42 (2× s, 2H, H4 and H8), 6.37 (dd, J = 10.9, 17.6 Hz, 1H, H2), 6.15 (t, J = 2.2 Hz, 1H, H6), 5.33 (dd, J = 1.0, 17.6, 1H, H_{trans}-1a), 5.04 (dd, J = 1.0, 10.9 Hz, 1H, H_{cis}-1b), 1.04 (s, 18H, 2× $(CH_3)_3$). ^{13}C-NMR (125 MHz, $CDCl_3$): δ 156.4, 139.0, 136.7, 135.6, 133.0, 129.9, 127.8, 113.8, 111.3, 111.1, 26.7, 19.6.

*2.2.3. p-Iodoanisole (**10**).* *p*-Iodoanisole (**10**) was prepared according to the literature procedure.[54] A mixture of 4-iodophenol (**9**) (264 mg, 1.2 mmol), methyl iodide (170 mg, 1.2 mmol), and K_2CO_3 (828 g, 6.0 mmol) in 10 mL of acetone was stirred at 60 °C for 24 h. After cooling to room temperature, the mixture was poured into 100 mL of water and extracted with diethyl ether (3 × 40 mL). The combined organic phase was evaporated under vacuum to remove the solvent. The residue was subjected to silica gel column chromatography, eluting with hexane to give *p*-iodoanisole (**10**) as white crystals (258 mg, 92%). ^{1}H-NMR (500 MHz, $CDCl_3$): δ 7.56 (d, J = 9.0 Hz, 2H), 6.68 (d, J = 9.0 Hz, 2H), 3.78 (s, 3H, CH_3). ^{13}C-NMR (125 MHz, $CDCl_3$): δ 159.5, 138.3, 116.5, 82.8, 55.4.

*2.2.4. 4′-O-Me-Resveratrol (**11**).* To a stirred solution of 3,5-di-*tert*-butyldiphenylsilyloxystyrene (**8**) (240 mg, 0.39 mmol) and *p*-iodoanisole (**10**) (110 mg, 0.47 mmol) in anhydrous dimethylformamide (5 mL) at room temperature under a nitrogen atmosphere were added benzyltriethylammonium chloride (90 mg, 0.39 mmol), tributylamine (241 μL, 1.01 mmol), and palladium (II) acetate (5 mg, 5 mol %). The resulting pale orange solution was stirred at 110 °C for 30 min and then allowed to cool to room temperature. The mixture was poured onto water (150 mL) and then extracted with diethyl ether (3 × 50 mL). The combined organic phase was washed with water (2 × 50 mL), then dried over anhydrous $MgSO_4$, and filtered, and the solvent evaporated under

DOI: 10.1021/acsomega.9b00722
ACS Omega 2019, 4, 8222−8230

vacuum. The residue was subjected to silica gel column chromatography, eluting with hexane/ethyl acetate (15:1) to give 3,5-di-*tert*-butyldiphenylsilyloxy-4′-*O*-Me-resveratrol as a pale brown crystal (276 mg, 98%). ^{1}H-NMR (500 MHz, acetone-d_6): δ 7.63−7.36 (m, 20H, Ph-H), 7.38 (d, J = 8.8 Hz, 2H, H2′ and H6′), 6.89 (d, J = 8.8 Hz , 2H, H3′ and H5′), 6.76 (d, J = 16.4 Hz, 1H, H8), 6.73 (d, J = 16.4 Hz, 1H, H7), 6.61 (2× s, 2H, H2 and H6), 6.16 (t, J = 2.2 Hz, 1H, H4), 3.78 (s, 3H, OCH_3), 1.02 (s, 18H, (2× $(CH_3)_3$). ^{13}C-NMR (125 MHz, acetone-d_6): δ 160.4, 157.3, 140.4, 136.2, 136.2, 133.4, 130.8, 128.7, 128.6, 126.6, 114.9, 111.9, 111.3, 55.5, 26.9, 19.9. The next step involved the deprotection of the TBDPS groups of 3,5-di-*tert*-butyldiphenylsilyloxy-4′-*O*-Me-resveratrol. To achieve that, TBAF trihydrate (1.0 M in THF) (1.9 mL, 1.88 mmol) was added to a cold (0 °C) and stirred solution of 3,5-di-*tert*-butyldiphenylsilyloxy-4′-*O*-Me-resveratrol (337 mg, 0.47 mmol) in THF (8 mL). After stirring for 1 h at 0 °C, saturated aqueous NH_4Cl solution (50 mL) was poured into the reaction mixture. The resultant mixture was extracted with ethyl acetate (3 × 150 mL). The combined organic phase was washed with saturated aqueous NH_4Cl solution (2 × 50 mL) and brine (2 × 50 mL). The aqueous phases were extracted with ethyl acetate (2 × 100 mL), and the combined organic phases were dried over $MgSO_4$. The solvent was evaporated under vacuum, and the residue was subjected to silica gel column chromatography, eluting with hexane/ethyl acetate (2:1) to give 4′-*O*-Me-resveratrol (**11**) as a pale brown crystal (109 mg, 96%). The ^{1}H-NMR and ^{13}C-NMR data are presented in Table 1.

2.3. Synthesis of Deoxyrhapontigenin-3-*O*-*β*-D-glucuronide (5).

2.3.1. (E)-1-[3-Hydroxy-5-O-(2,3,4-tri-O-acetyl-β-D-glucopyranoside)phenyl]-2-(4′-methoxy) Ethene Methyl Ester (12). A suspension of the dried 4′-*O*-Me-resveratrol (**11**) (120 mg, 0.49 mmol), 2,3,4-tri-*O*-acetyl-*α*-D-glucuronic acid methyl ester, tricholoroacetamidate (296 mg, 0.59 mmol), and 4 Å MS (2.0 g) in anhydrous CH_2Cl_2 (10 mL) was vigorously stirred at room temperature for 30 min. The suspension was then cooled to 0 °C, and a solution of the Lewis acid [TMSOTf (22 μL in 1.4 mL of CH_2Cl_2) or $BF_3{\cdot}OEt_2$ (42 μL in 2.7 mL of CH_2Cl_2)] was slowly added. The resulting suspension was continuously stirred at 0 °C for 3 h (in the case of TMSOTf) or 5 h (in the case of $BF_3{\cdot}OEt_2$). Then, the reaction was quenched with three drops of Et_3N and filtered under Celite, and the solvent was removed under vacuum. The residue was purified by silica gel column chromatography, eluting with hexane/ethyl acetate (4:5) to give (*E*)-1-[3-hydroxy-5-*O*-(2,3,4-tri-*O*-acetyl-*β*-D-glucopyranoside)phenyl]-2-(4′-methoxy) ethene methyl ester (**12**) as a colorless oil [83 mg, 30% (TMSOTf) and 97 mg, 35% ($BF_3{\cdot}OEt_2$)]. 4′-*O*-Me-Resveratrol (**11**) was recovered from both reaction conditions [78 mg (TMSOTf) and 60 mg ($BF_3{\cdot}OEt_2$)]. ^{1}H-NMR (500 MHz, acetone-d_6): δ 8.36 (d, J = 8.7 Hz, 2H, H2′ and H6′), 7.96 (d, J = 16.4 Hz, 1H, H8), 7.83 (d, J = 16.4 Hz, 1H, H7), 7.80 (d, J = 8.7 Hz, 2H, H3′ and H5′), 7.64 and 7.62 (dt, 2H, J = 1.7 Hz, H2 and H6), 7.31 (t, J = 2.2 Hz, 1H, H4), 6.41 (d, 1H, H1″), 6.32 (t, 1H), and 6.05−6.09 (m, 3H, H2″, H3″, H4″), 5.46 (d, 1H, H5″), 4.67 (s, 3H, C4′OCH_3), 4.55 (s, 3H, OCH_3-glucuronic moiety), 2.89, 2.86, 2.85 (3× s, 3× (3H), OAc-glucuronic moiety).^{13}C-NMR (125 MHz, acetone-d_6): δ 170.2, 169.9, 169.7, 167.9, 160.5, 159.5, 159.2, 141.1, 130.7, 129.7, 128.7, 126.7, 114.9, 109.1, 106.7, 103.9, 99.2, 72.8, 72.5, 71.8, 70.3, 55.6, 53.0, 20.6, 20.5, 20.4.

2.3.2. Deoxyrhapontigenin-3-O-β-D-glucuronide (5). To a stirred solution of (*E*)-1-[3-hydroxy-5-*O*-(2,3,4-tri-*O*-acetyl-*β*-D-glucopyranoside)phenyl]-2-(4′-methoxy) ethene methyl ester (**12**) (45 mg, 0.08 mmol) in tetrahydrofuran (THF) and methanol (4:1, v/v) (15 mL) at 0 °C under a nitrogen atmosphere was added sodium methoxide [5.4 M (30 wt.%) in methanol] (0.65 mL, 3.51 mmol). After stirring for 1 h at 0 °C, sodium hydroxide (1.0 M in water) (13.3 mL, 1.3 mmol) was added to the reaction mixture. The resulting pale-yellow solution was stirred at 0 °C for 2.5 h. Amberlyst 15 hydrogen form was then added to adjust the reaction mixture to pH 4. The resin was filtered off and washed with methanol (3 × 20 mL), and the solvent was evaporated under air flow to a thick brown oil. The oil was subjected to preparative HPLC to give deoxyrhapontigenin-3-*O*-*β*-D-glucuronide (**5**) as a white solid (27 mg, 80%). The ^{1}H-NMR and ^{13}C-NMR data are presented in Table 2. Melting point of **5**: decomposes without melting above 250 °C. Preparative HPLC was performed on an Agilent HP1200 HPLC, monitoring at 280 nm. HPLC with ChemStation software version B.02.01.SRI was equipped with a G1322A degasser, G1311A quaternary pump, a

Table 2. ^{1}H-NMR (500 MHz) and ^{13}C-NMR (125 MHz), in MeOD-d_4, of Deoxyrhapontigenin-3-*O*-*β*-D-glucuronide (5)

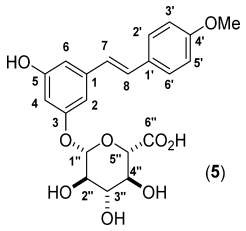

atom #	^{1}H-NMR (δ ppm, J Hz) (500 MHz)	lit.[a]	^{13}C-NMR (δ ppm) (125 MHz)	lit.[a]
1			141.2	141.1
2	6.78, br. t	6.78, br.t	107.5	107.2
3			160.5	159.2
4	6.50, t, J = 2.1	6.45, t, J = 1.9	104.4	104.1
5			159.9	159.8
6	6.64, br. t	6.65, br.t	108.4	108.7
7	6.92, d, J = 16.3	6.89, d, J = 16.5	127.4	127.4
8	7.02, d, J = 16.3	7.04, d, J = 16.5	129.6	129.6
1′			131.4	[b]
2′	7.45, d, J = 8.8	7.45, d, J = 8.5	128.8	130.8
3′	6.91, d, J = 8.9	6.89, d, J = 8.5	115.1	128.4
4′			160.9	114.9
5′	6.91, d, J = 8.9	6.89, d, J = 8.5	115.1	160.5
6′	7.45, d, J = 8.8	7.45, d, J = 8.5	128.8	114.9
OCH_3	3.80, s	3.80, s	55.7	128.4
1″	4.92[c]	4.96, d, J = 7.2	102.6	55.6
2″	3.53−3.47, m	3.50, m	74.7[d]	102.5
3″	3.53−3.47, m	3.51, t, d, J = 9.1	77.7[d]	76.9
4″	3.57, m	3.79, m	73.4	74.4
5″	3.83, d, J = 9.6	4.00, d, d, J = 9.5	76.6	72.5
6″			167.4	76.5
OH	8.31, s			

[a]Ref 52. [b]The ^{13}C-NMR for H1′ was not furnished by the authors, potentially leading to misplaced assignments. [c]The signal for the anomeric hydrogen (H1″) was partially superimposed on the solvent signal. [d]These signals may be inverted due to the uncertainty of assignment.

DOI: 10.1021/acsomega.9b00722
ACS Omega 2019, 4, 8222−8230

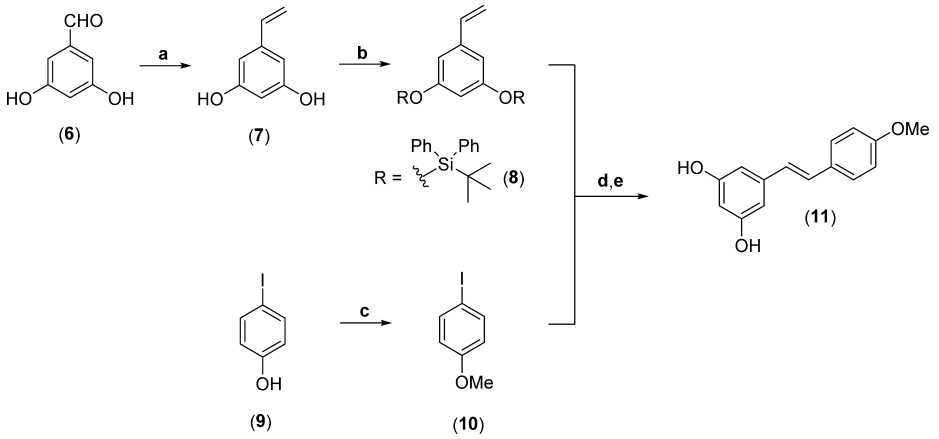

Figure 2. Synthetic route to 4′-*O*-Me-resveratrol (**11**) by Heck coupling between 3,5-dihydroxybenzaldehyde (**6**) and *p*-iodoanisole (**10**). Reagents and reaction conditions: (a) NaH, $CH_3P(C_6H_5)_3Br$, DMSO, 70 °C (1 h), then r.t. (1 h) (91%); (b) imidazole, *tert*-butyl(chloro)diphenylsilane (TBDPSCl) (**8**), DMF, 18 h (95%); (c) CH_3I, K_2CO_3, acetone, 60 °C, 24 h (92%); (**d**) $BnEt_3NCl$, Bu_3N, $Pd(OAc)_2$, DMF, 110 °C, 30 min (98%); (**e**) TBAF trihydrate (1.0 M in THF), THF, 0 °C (96%).

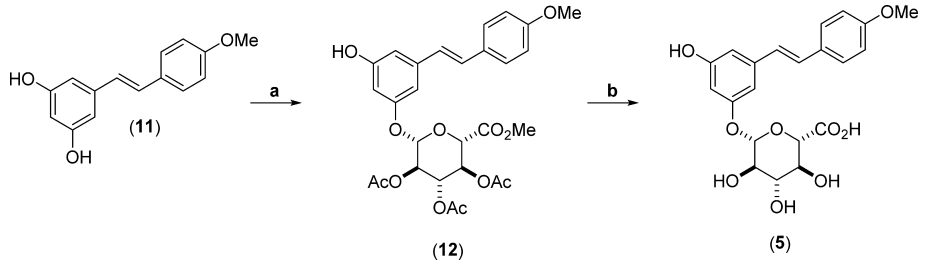

Figure 3. Preparation of deoxyrhapontigenin-3-*O*-*β*-D-glucuronide (**5**) from 4′-*O*-Me-resveratrol (**11**).

G1367B autosampler, G1316A thermostatic column compartment, and G1315C diode array detector. A Phenomenx Luna 10 μm C18(2) 250 × 21.2 mm column was used for preparative HPLC on the Agilent HPLC system. The column was eluted with an isocratic mixture of acetonitrile and water with formic acid (0.1%) (28:72, v/v). The flow rate was set at 8 mL/min, and the peak related to deoxyrhapontigenin-3-*O*-*β*-D-glucuronide (**5**) was detected at 37 min.

3. RESULTS AND DISCUSSION

To ultimately address biological mechanisms whereby brain-bioavailable deoxyrhapontigenin-3-*O*-*β*-D-glucuronide (**5**) may impact the development of AD, we investigated the synthesis of **5** from 4-*O*-Me-resveratrol (**11**) (Figures 2 and 3).

4-*O*-Me-Resveratrol (**11**) was obtained through the Heck coupling between the 3,5-di-*tert*-butyldiphenylsilyloxystyrene (**8**) and *p*-iodoanisole (**10**) (Figure 2). Styrene **8** was prepared, with 86% yield (two steps), through Wittig reaction between 3,5-dihydroxybenzaldehyde (**6**) and methyltriphenylphosphonium bromide according to the methodology developed by Farina et al.,[53] followed by the protection of hydroxyl groups with *tert*-butyl(chloro)diphenylsilane (TBDPSCl) (Figure 2). Protection of the hydroxyl groups of **7** was necessary, but it is well known that if styrenes are unprotected, or protected with acetyl or *tert*-butyldimethylsilyl (TBDMS), desired products are obtained with low yields.[53,55] For this reason, we selected *tert*-butyldiphenylsilyl (TBDPS) as a protecting group since this group is known to be more stable than TBDMS under both alkaline and acid conditions.[56,57] Synthesis of *p*-iodoanisole (**10**) was achieved with 92% yield as described by Chen et al.[54] To our satisfaction, the Heck coupling between **8** and **10** furnished 3,5-di-*tert*-butyldiphenylsilyloxy-4′-*O*-Me-resveratrol with 98% yield, and no non-TBDPS-protected adducts and/or (*Z*)-isomer were isolated from the reaction medium. The yield of the Heck reaction (98%) was more than 2-fold higher than obtained by Farina et al.[53] and Hoshino et al.,[58] who used the 3,5-di-*tert*-butyldimethylsilyloxystyrene (a TBDMS analogue of **8**) as the olefin and acetyliodophenol (an acetyl analogue of **10**) for the reaction. Finally, the deprotection of the TBDPS protection groups using 1.0 M TBAF trihydrate solution in THF-furnished 4-*O*-Me-resveratrol (**11**) with 96% yield.

Using our synthetic approach, the 4-*O*-Me-resveratrol (**11**) was stereoselectively obtained from 3,5-dihydroxybenzaldehyde (**6**) in four steps, 81% yield and excellent purity (HPLC, >98%; Figure 20SA, Supporting Information). To the best of our knowledge, our synthetic approach is one of the most efficient routes to prepare 4-*O*-Me-resveratrol (**11**). For example, Mizuni et al.[59] reported the preparation of 4-*O*-Me-resveratrol (**11**) using a Wittig reaction as the key step. Compound **11** was obtained in three steps, however, with only 7% overall yield.[59] Under the Wittig reaction conditions, the (*E*)-isomer of **11** was formed as the minor regioisomer (1.0:2.8, *E*/*Z*),[59] similar to the 1.0:2.3 *E*/*Z* ratio reported by Orsini et al.[60] but considerably higher than the 1.0:9.0 *E*/*Z* ratio described by Pettit et al.[61] Šmidrkal et al.[62] reported a highly stereoselective synthesis of 4-*O*-Me-resveratrol (**11**) [only the (*E*)-isomer was observed] in seven steps. These authors employed the Wittig−Horner reaction, a well-known reaction for producing predominantly *E*-alkenes, as the key step for obtaining the desired compound **11**; however, the overall yield for **11** was very low (4%).[62] The Wittig−Horner

DOI: 10.1021/acsomega.9b00722
ACS Omega 2019, 4, 8222−8230

reaction was used as a key step for synthesis of 4-*O*-Me-resveratrol (**11**) from 3,5-dihydroxybenzoic acid. The authors obtained 4-*O*-Me-resveratrol (**11**) in six steps, with 24% overall yield and 100% stereoselectivity for the (*E*)-isomer.[63,64]

The ^{1}H-nuclear magnetic resonance (^{1}H-NMR) and ^{13}C-NMR spectra for all synthesized compounds shown in Figure 2 are available as Figures 1S−10S (Supporting Information). The ^{1}H-NMR and ^{13}C-NMR and liquid chromatography coupled to mass spectrometry (LC/MS) data derived from 4′-*O*-Me-resveratrol (**11**) were in complete accordance with the assigned structure of **11** and those already published in the literature (Table 1).[52] The geometry of the double bond was assigned as *E* for **11** based on the coupling constant of the signals for the olefinic protons H7 and H8 ($J_{7,8}$ = 15.9 Hz). This value is consistent with those reported elsewhere by Pettit et al.[61] ($J_{7,8}$ = 15.9 Hz), Orsini et al.[60] ($J_{7,8}$ = 16.4 Hz), and Lee et al.[64] ($J_{7,8}$ = 16.5 Hz). Finally, the LC−MS analysis of 4′-*O*-Me-resveratrol (**11**) (Figure 20SB, Supporting Information) showed the expected quasimolecular ion at *m*/*z* 241.1 [M − H]$^{-}$ (calcd for **11**, 241.2).

The next step was the glucuronidation of 4′-*O*-Me-resveratrol (**11**), which can be difficult because of the very low reactivity of phenolic hydroxyl groups as a glucuronic acid acceptor.[60] First, we tried to perform the glucuronidation of **11** under two different basic conditions: (i) acetobromo-α-D-glucuronic acid methyl ester, Ag_2O, piridine, 3 Å molecular sieves, 0 °C, 48 h[65] or (ii) acetobromo-α-D-glucuronic acid methyl ester, Ag_2CO_3, THF, 4 Å molecular sieves, 0 °C, 24 h.[66] However, under both conditions, the desired glucuronide **12** was not formed, and unreacted 4′-*O*-Me-resveratrol (**11**) was recovered from the reaction mixture. Due to the lack of success in obtaining **12** using basic conditions, we attempted to perform the glucuronidation of **11** (Figure 3) using trimethylsilyltrifluoromethanesulfonate (TMSOTf) and boron trifluoride diethyl etherate ($BF_3{\cdot}OEt_2$), two Lewis acids that are well known to catalyze the glucuronidation of phenolic compounds.[67,68] Under these acidic conditions, the desired glucuronide **12** was obtained in approximately 30 and 35% yields when TMSOTf or $BF_3{\cdot}OEt_2$ were used as Lewis acid, respectively (Figure 3). Thereafter, deprotection of the acetyl groups, as well as the hydrolysis of the methyl ester, was easily achieved using a mixture of 5.4 M MeONa in MeOH and 1.0 M NaOH in water at 0 °C for 3.5 h (Figure 3). Acid workup using Amberlyst 15 hydrogen form to adjust the pH to 3.0, followed by evaporation of the solvent and purification of the residue by preparative HPLC, furnished deoxyrhapontigenin-3-*O*-β-D-glucuronide (**5**) with 80% yield and excellent purity (HPLC, >99%; Figure 1S, Supporting Information) from **5**. Overall, our synthetic approach furnished the deoxyrhapontigenin-3-*O*-β-D-glucuronide (**5**) from 3,5-dihydroxybenzaldehyde (**6**) in six steps, 21% yield, and excellent purity.

Deoxyrhapontigenin-3-*O*-β-D-glucuronide (**5**) showed a quasimolecular ion at *m*/*z* 417.0 [M − H]$^{-}$ (calcd for **5**, 417.2). A fragment at *m*/*z* 241 for **5** (Figure 22SB, Supporting Information) was also observed, corresponding to the neutral loss of 176 Da (the glucuronic moiety) from the quasimolecular precursor ions *m*/*z* 417 [M − H]$^{-}$, indicating that **5** is a glucuronide conjugate of **11**. The same pattern of fragmentation was observed for dihydroresveratrol-3-*O*-β-D-glucuronide, an analogue of **5**.[69]

Complete assignments of the hydrogen and carbon atoms of both the aromatic rings and glucuronic acid moiety were accomplished using heteronuclear multiple quantum coherence (HMQC) and heteronuclear multiple bond coherence (HMBC) (Table 2) and are in accordance to those previously described by Marvalin and Azerad,[52] except for some of the ^{13}C-NMR assignments (Table 2). The ^{1}H-NMR spectrum of **5**, in comparison with that of **11**, showed that H2 and H6, which are identical in **11**, became discriminated in the glucuronide **5**, as indicated by the multiplicity of the signals at 6.78 and 6.64 ppm for H2 and H6, respectively (Table 2), suggesting that the glucuronidation broke the symmetry of the molecule. The $J_{7,8}$ value of 16.3 Hz for **5** confirmed the *E* stereochemistry of the stilbene bridge and agrees with the value reported by Marvalin and Azerad[52] ($J_{7,8}$ = 16.5 Hz) and Lucas et al.[70] ($J_{7,8}$ = 16.4 Hz). The anomeric hydrogen H1″ (δ_H 4.92 ppm) was partially superimposed on the solvent signal; however, it was possible to determine its anomeric carbon C3 at δ_C 160.5 ppm. Both assignments are consistent with those reported by Marvalin and Azerad.[52] The main discrepancies between our ^{13}C-NMR data and those reported by Marvalin and Azerad[52] are related to the assignments for the carbon of the aromatic ring that bears the OMe group (C1′ to C6′) and the glucuronic acid unit (C1″ to C6″) (Table 2). The anomeric carbon (C1″) of the glucuronic acid moiety appears around δ_C 102 ppm, consistent with the literature data;[68−70] however, this is very different from the δ_C 55.6 ppm reported by Marvalin and Azerad.[52] The assignments of proton-bearing carbons (OCH_3, C2, C6, C4, C2′, C3′, C5′, C6′, C1″, C2″, C3″, C4″, and C5″) were achieved using HMQC. The assignments of the ipso carbons C1, C3, C5, C1′, and C4′ were accomplished using HMBC. Specifically, C1 was assigned based on its three-bond coupling with H8, whereas C3 and C5 were assigned based on their two-bond correlation with H2/H4 and H4/H6, respectively. It is worth mentioning that C3, to which the *O*-glucuronic acid residue is attached, also has a three-bond long-range coupling with the anomeric H1″. C1′ was assigned on the basis of its three-bond coupling with H3′, H5′, and H7, whereas C4′ was assigned on the basis of its three-bond coupling with H2′ and H6′. In addition, C4′ showed strong three-bond coupling with the methyl hydrogen (δ_H 3.80 ppm). Thus, by the combination of HSQC and HMBC, all carbons could be assigned unambiguously.

4. CONCLUSIONS

As outlined here, we described the synthesis of 4-*O*-Me-resveratrol (**2**) in four steps with 74% overall yield and present what we believe to be the first report of the chemical synthesis of deoxyrhapontigenin-3-*O*-β-D-glucuronide (**5**), obtained in six steps with 21% overall yield. The robust synthetic approach for **5** will allow us and others to evaluate the mechanism of action of this brain-targeted bioactive dietary glucuronide in the modulation of AD and other neurological disorders by resveratrol (**1**).

■ ASSOCIATED CONTENT

Supporting Information

The Supporting Information is available free of charge on the ACS Publications website at DOI: 10.1021/acsomega.9b00722.

^{1}H-NMR and ^{13}C-NMR spectra of 3,5-dihydroxystyrene, ^{1}H-NMR and ^{13}C-NMR spectra of 3,5-di-*tert*-butyldiphenylsilyloxystyrene, ^{1}H-NMR and ^{13}C-NMR spectra of *p*-iodoanisole, ^{1}H-NMR and ^{13}C-NMR spectra of (*E*)-(5-(4-methoxystyryl)-1,3-phenylene)bis-

DOI: 10.1021/acsomega.9b00722
ACS Omega 2019, 4, 8222−8230

(methyldiphenylsilane), ^{1}H-NMR and ^{13}C-NMR spectra of 4′-*O*-Me-resveratrol, ^{1}H-NMR and ^{13}C-NMR spectra of (*E*)-1-[3-hydroxy-5-*O*-(2,3,4-tri-*O*-acetyl-*β*-D-glucopyranoside)phenyl]-2-(4′-methoxy) ethene methyl ester, ^{1}H-NMR and ^{13}C-NMR spectra of deoxyrhapontigenin-3-*O*-*β*-D-glucuronide, HMQC-NMR spectra of deoxyrhapontigenin-3-*O*-*β*-D-glucuronide, HMBC-NMR spectra of deoxyrhapontigenin-3-*O*-*β*-D-glucuronide, LC−MS/MS analysis of 4′-*O*-Me-resveratrol, LC−MS/MS analysis of deoxyrhapontigenin-3-*O*-*β*-D-glucuronide, and MS and MS/MS spectra of deoxyrhapontigenin-3-*O*-*β*-D-glucuronide (PDF)

AUTHOR INFORMATION

Corresponding Authors

*E-mail: adefatima@qui.ufmg.br (A.d.F.).
*E-mail: Richard.Dixon@unt.edu (R.A.D).

ORCID

Ângelo de Fátima: 0000-0003-2344-5590
Giulio M. Pasinetti: 0000-0002-1524-5196
Richard A. Dixon: 0000-0001-8393-9408

Notes

The authors declare no competing financial interest.

ACKNOWLEDGMENTS

This study was supported by grant number P50 AT008661-01 from the NCCIH and the ODS and by the University of North Texas. G.M.P. holds a Senior VA Career Scientist Award. A.d.F. acknowledges the Brazilian National Council for Scientific and Technological Development (CNPq) for the scholarship received during his sabbatical year (process #204106/2017-6) at the University of North Texas, Denton, TX, USA. The authors acknowledge the BioAnalytical Facility at the University of North Texas for the support with mass spectrometry analyses during this work. We acknowledge that the contents of this study do not represent the views of the NCCIH, the ODS, the NIH, the U.S. Department of Veterans Affairs, or the United States Government.

REFERENCES

(1) Ness, A. R.; Powles, J. W. Fruit and vegetables, and cardiovascular disease: A review. *Int. J. Epidemiol.* **1997**, *26*, 1−13.
(2) Kris-Etherton, P. M.; Hecker, K. D.; Bonanome, A.; Coval, S. M.; Binkoski, A.E.; Hilpert, K. F.; Griel, A. E.; Etherton, T. D. Bioactive compounds in foods: Their role in the prevention of cardiovascular disease and cancer. *Am. J. Med.* **2002**, *113*, 71−88.
(3) Yao, L. H.; Jiang, Y. M.; Shi, J.; Tomas-Barberan, F. A.; Datta, N.; Singanusong, R.; Chen, S. S. Flavonoids in food and their health benefits. *Plant Foods Hum. Nutr.* **2004**, *59*, 113−122.
(4) Shao, Y.; Bao, J. Polyphenols in whole rice grain: Genetic diversity and health benefits. *Food Chem.* **2015**, *180*, 86−97.
(5) Costa, C.; Tsatsakis, A.; Mamoulakis, C.; Teodoro, M.; Briguglio, G.; Caruso, E.; Dimitris, T.; Margina, D.; Dardiotis, E.; Kouretas, D.; Fenga, C. Current evidence on the effect of dietary polyphenols intake on chronic diseases. *Food Chem. Toxicol.* **2017**, *110*, 286−299.
(6) Gürbüz, N.; Uluişik, S.; Frary, A.; Frary, A.; Doğanlar, S. Health benefits and bioactive compounds of eggplant. *Food Chem.* **2018**, *268*, 602−610.
(7) Sanlier, N.; Atik, İ.; Atik, A. A minireview of effects of white tea consumption on diseases. *Trends Food Sci. Technol.* **2018**, *82*, 82−88.
(8) Stahl, W.; van den Berg, H.; Arthur, J.; Bast, A.; Dainty, J.; Faulks, R. M.; Gärtner, C.; Haenen, G.; Hollman, P.; Holst, B.; Kelly, F. J.; Polidori, M. C.; Rice-Evans, C.; Southons, S.; van, V. T.; Viña-Ribes, J.; Williamson, G.; Astley, S. B. Bioavailability and metabolism. *Mol. Aspects Med.* **2002**, *23*, 39−100.
(9) Walle, T. Bioavailability of resveratrol. *Ann. N. Y. Acad. Sci.* **2011**, *1215*, 9−15.
(10) Chiou, Y. S.; Wu, J. C.; Huang, Q.; Shahidi, F.; Wang, Y. J.; Ho, C. T.; Pan, M. H. Metabolic and colonic microbiota transformation may enhance the bioactivities of dietary polyphenols. *J. Funct. Foods* **2014**, *7*, 3−25.
(11) De Vries, K.; Strydom, M.; Steenkamp, V. Bioavailability of resveratrol: Possibilities for enhancement. *J. Herb. Med.* **2018**, *11*, 71−77.
(12) Pannu, N.; Bhatnagar, A. Resveratrol: From enhanced biosynthesis and bioavailability to multitargeting chronic diseases. *Biomed. Pharmacother.* **2019**, *109*, 2237−2251.
(13) Scalbert, A.; Williamson, G. Dietary intake and bioavailability of polyphenols. *J. Nutr.* **2000**, *130*, 2073S−2085S.
(14) Monagas, M.; Urpi-Sarda, M.; Sánchez-Patán, F.; Llorach, R.; Garrido, I.; Gómez-Cordovés, C.; Andres-Lacueva, C.; Bartolomé, B. Insights into the metabolism and microbial biotransformation of dietary flavan-3-ols and the bioactivity of their metabolites. *Food Funct.* **2010**, *1*, 233−253.
(15) Delmas, D.; Aires, V.; Limagne, E.; Dutartre, P.; Mazué, F.; Ghiringhelli, F.; Latruffe, N. Transport, stability, and biological activity of resveratrol. *Ann. N. Y. Acad. Sci.* **2011**, *1215*, 48−59.
(16) Ho, L.; Ferruzzi, M. G.; Janle, E. M.; Wang, J.; Gong, B.; Chen, T. Y.; Lobo, J.; Cooper, B.; Wu, Q. L.; Talcott, S. T.; Percival, S. S.; Simon, J.E.; Pasinetti, G. M. Identification of brain-targeted bioactive dietary quercetin-3-*O*-glucuronide as a novel intervention for Alzheimer's disease. *FASEB J.* **2013**, *27*, 769−781.
(17) Fulda, S. Resveratrol and derivatives for the prevention and treatment of cancer. *Drug Discovery Today* **2010**, *15*, 757−765.
(18) Alamolhodaei, N. S.; Tsatsakis, A. M.; Ramezani, M.; Hayes, A. W.; Karimi, G. Resveratrol as MDR reversion molecule in breast cancer: An overview. *Food Chem. Toxicol.* **2017**, *103*, 223−232.
(19) Elshaer, M.; Chen, Y.; Wang, X.J.; Tang, X. Resveratrol: An overview of its anti-cancer mechanisms. *Life Sci.* **2018**, *207*, 340−349.
(20) Szkudelska, K.; Szkudelski, T. Resveratrol, obesity and diabetes. *Eur. J. Pharmacol.* **2010**, *635*, 1−8.
(21) Szkudelski, T.; Szkudelska, K. Resveratrol and diabetes: From animal to human studies. *Biochim. Biophys. Acta* **2015**, *1852*, 1145−1154.
(22) Öztürka, E.; Arslan, A. K. K.; Yerer, M. B.; Bishayee, A. Resveratrol and diabetes: A critical review of clinical studies. *Biomed. Pharmacother.* **2017**, *95*, 230−234.
(23) Kim, S.; Jin, Y.; Choi, Y.; Park, T. Resveratrol exerts anti-obesity effects via mechanisms involving down-regulation of adipogenic and inflammatory processes in mice. *Biochem. Pharmacol.* **2011**, *81*, 1343−1351.
(24) de Ligt, M.; Timmers, S.; Schrauwen, P. Resveratrol and obesity: Can resveratrol relieve metabolic disturbances? *Biochim. Biophys. Acta* **2015**, *1852*, 1137−1144.
(25) Mahal, H. S.; Mukherjee, T. Scavenging of reactive oxygen radicals by resveratrol: Antioxidant effect. *Res. Chem. Intermed.* **2006**, *32*, 59−71.
(26) Gülçin, I. Antioxidant properties of resveratrol: A structure-activity insight. *Innovative Food Sci. Emerging Technol.* **2010**, *11*, 210−218.
(27) Hussein, M. A. A convenient mechanism for the free radical scavenging activity of resveratrol. *Int. J. Phytomed.* **2011**, *3*, 459−469.
(28) Gerszon, J.; Rodacka, A.; Puchała, M. Antioxidant properties of resveratrol and its protective effects in neurodegenerative diseases. *Adv. Cell Biol.* **2014**, *4*, 97−117.
(29) Alarcon De La Lastra, C.; Villegas, I. Resveratrol as an anti-inflammatory and anti-aging agent: Mechanisms and clinical implications. *Mol. Nutr. Food Res.* **2005**, *49*, 405−430.
(30) Udenigwe, C. C.; Ramprasath, V. R.; Aluko, R. E.; Jones, P. J. Potential of resveratrol in anticancer and anti-inflammatory therapy. *Nutr. Rev.* **2008**, *66*, 445−454.

DOI: 10.1021/acsomega.9b00722
ACS Omega 2019, 4, 8222−8230

(31) Poulsen, M. M.; Fjeldborg, K.; Ornstrup, M. J.; Kjær, T. N.; Nøhr, M. K.; Pedersen, S. B. Resveratrol and inflammation: Challenges in translating pre-clinical findings to improved patient outcomes. *Biochim. Biophys. Acta* **2015**, *1852*, 1124−1136.
(32) Anekonda, T. S. Resveratrol - A boon for treating Alzheimer's disease? *Brain Res. Rev.* **2006**, *52*, 316−326.
(33) Villaflores, O. B.; Chen, Y. J.; Chen, C. P.; Yeh, J. M.; Wu, T. Y. Curcuminoids and resveratrol as anti-Alzheimer agents. *Taiwanese J. Obstetr. Gynecol.* **2012**, *51*, 515−525.
(34) Bastianetto, S.; Ménard, C.; Quirion, R. Neuroprotective action of resveratrol. *Biochim. Biophys. Acta* **2015**, *1852*, 1195−1201.
(35) Drygalski, K.; Fereniec, E.; Koryciński, K.; Chomentowski, A.; Kiełczewska, A.; Odrzygóźdź, C.; Modzelewska, B. Resveratrol and Alzheimer's disease. From molecular pathophysiology to clinical trials. *Exp. Gerontol.* **2018**, *113*, 36−47.
(36) Storniolo, C. E.; Moreno, J. J. Resveratrol metabolites have an antiproliferative effect on intestinal epithelial cancer cells. *Food Chem.* **2012**, *134*, 1385−1391.
(37) Patel, K. R.; Brown, V. A.; Jones, D. J.; Britton, R. G. Clinical pharmacology of resveratrol and its metabolites in colorectal cancer patients. *Cancer Res.* **2010**, *70*, 7392−7399.
(38) Aires, V.; Limagne, E.; Cotte, A. K.; Latruffe, N.; Ghiringhelli, F.; Delmas, D. Resveratrol metabolites inhibit human metastatic colon cancer cells progression and synergize with chemotherapeutic drugs to induce cell death. *Mol. Nutr. Food Res.* **2013**, *57*, 1170−1181.
(39) Lasa, A.; Churruca, I.; Eseberri, I.; Andrés-Lacueva, C.; Portillo, M. P. Delipidating effect of resveratrol metabolites in 3T3-L1 adipocytes. *Mol. Nutr. Food Res.* **2012**, *56*, 1559−1568.
(40) Kaldas, M. I.; Walle, U. K.; Walle, T. Resveratrol transport and metabolism by human intestinal Caco-2 cells. *J. Pharm. Pharmacol.* **2003**, *55*, 307−312.
(41) Walle, T.; Hsieh, F.; DeLegge, M. H.; Oatis, J. E.; Walle, K. High absorption but very low BIOAVAILABILITY of oral resveratrol in humans. *Drug Metab. Dispos.* **2004**, *32*, 1377−1382.
(42) Juan, M. E.; Maijó, M.; Planas, J. M. Quantification of trans-resveratrol and its metabolites in rat plasma and tissues by HPLC. *J. Pharm. Biomed. Anal.* **2010**, *51*, 391−398.
(43) Spencer, J. P. The impact of flavonoids on memory: physiological and molecular considerations. *Chem. Soc. Rev.* **2009**, *38*, 1152−1161.
(44) Rezai-Zadeh, K.; Shytle, D.; Sun, N.; Mori, T.; Hou, H.; Jeanniton, D.; Ehrhart, J.; Townsend, K.; Zeng, J.; Morgan, D.; Hardy, J.; Town, T.; Tan, J. Green tea epigallocatechin-3-gallate (EGCG) modulates amyloid precursor protein cleavage and reduces cerebral amyloidosis in Alzheimer transgenic mice. *J. Neurosci.* **2005**, *25*, 8807−8814.
(45) Hartman, R. E.; Shah, A.; Fagan, A. M.; Schwetye, K. E.; Parsadanian, M.; Schulman, R. N.; Finn, M. B.; Holtzman, D. M. Pomegranate juice decreases amyloid load and improves behavior in a mouse model of Alzheimer's disease. *Neurobiol. Dis.* **2006**, *24*, 506−515.
(46) Wang, J.; Ho, L.; Zhao, Z.; Seror, I.; Humala, N.; Dickstein, D. L.; Thiyagarajan, M.; Percival, S. S.; Talcott, S. T.; Pasinetti, G. M. Moderate consumption of Cabernet Sauvignon attenuates Aβ neuropathology in a mouse model of Alzheimer's disease. *FASEB J.* **2006**, *20*, 2313−2320.
(47) Vingtdeux, V.; Dreses-Werringloer, U.; Zhao, H.; Davies, P.; Marambaud, P. Therapeutic potential of resveratrol in Alzheimer's disease. *BMC Neurosci.* **2008**, *9*, S6.
(48) Wang, J.; Ho, L.; Zhao, W.; Ono, K.; Rosensweig, C.; Chen, L.; Humala, N.; Teplow, D. B.; Pasinetti, G. M. Grape-derived polyphenolics prevent A Oligomerization and attenuate cognitive deterioration in a mouse model of Alzheimer's disease. *J. Neurosci.* **2008**, *28*, 6388−6392.
(49) Thomas, P.; Wang, Y. J.; Zhong, J. H.; Kosaraju, S.; O'Callaghan, N. J.; Zhou, X. F.; Fenech, M. Grape seed polyphenols and curcumin reduce genomic instability events in a transgenic mouse model for Alzheimer's disease. *Mutat. Res., Fund. Mol. Mech. Mutagen.* **2009**, *661*, 25−34.
(50) Pasinetti, G. M. Novel role of red wine-derived polyphenols in the prevention of Alzheimer's disease dementia and brain pathology: Experimental approaches and clinical implications. *Planta Med.* **2012**, *78*, 1614−1619.
(51) Wang, J.; Bi, W.; Cheng, A.; Freire, D.; Vempati, P.; Zhao, W.; Gong, B.; Janle, E. M.; Chen, T. Y.; Ferruzi, M. G.; Schmeider, J.; Ho, L.; Pasinetti, G. M. Targeting multiple pathogenic mechanisms with polyphenols for the treatment of Alzheimer's disease - Experimental approach and therapeutic implications. *Front. Aging Neurosci.* **2014**, *6*, 42.
(52) Marvalin, C.; Azerad, R. Microbial glucuronidation of polyphenols. *J. Mol. Cat. B: Enzym.* **2011**, *73*, 43−52.
(53) Farina, A.; Ferranti, C.; Marra, C. An improved synthesis of resveratrol. *Nat. Prod. Res.* **2007**, *20*, 247−252.
(54) Chen, J.; Ko, S.; Liu, L.; Sheng, Y.; Han, H.; Li, X. The effect of different alkyl chains on the photovoltaic performance of D-π-A porphyrin-sensitized solar cells. *New J. Chem.* **2015**, *39*, 3736−3746.
(55) Learmonth, D. A. A concise synthesis of the 3-*O*-β-D- and 4'-*O*-β-d-Glucuronide conjugates oftrans-Resveratrol. *Bioconjugate Chem.* **2003**, *14*, 262−267.
(56) Hanessian, S.; Lavallee, P. The preparation and synthetic Utility oftert-Butyldiphenylsilyl ethers. *Can. J. Chem.* **1975**, *53*, 2975−2977.
(57) Torisawa, Y.; Shibasaki, M.; Ikegami, S. Novel reactivities on *tert*-butyldimethylsilyl and *tert*-butyldiphenylsilyl ethers; Application to the synthesis of $_{11\text{-epi-PGF2.ALPHA}}$. *Chem. Pharm. Bull.* **1983**, *31*, 2607−2615.
(58) Hoshino, J.; Park, E.-J.; Kondratyuk, T. P.; Marler, L.; Pezzuto, J. M.; van Breemen, R. B.; Mo, S.; Li, Y.; Cushman, M. Selective synthesis and biological evaluation of sulfate-conjugated resveratrol metabolites. *J. Med. Chem.* **2010**, *53*, 5033−5043.
(59) Mizuno, C. S.; Ma, G.; Khan, S.; Patny, A.; Avery, M. A.; Rimando, A. M. Design, synthesis, biological evaluation and docking studies of pterostilbene analogs inside PPARα. *Bioorg. Med. Chem.* **2008**, *16*, 3800−3808.
(60) Orsini, F.; Pelizzoni, F.; Bellini, B.; Miglierini, G. Synthesis of biologically active polyphenolic glycosides (combretastatin and resveratrol series). *Carbohydr. Res.* **1997**, *301*, 95−109.
(61) Pettit, G. R.; Grealish, M. P.; Jung, M. K.; Hamel, E.; Pettit, R. K.; Chapuis, J.-C.; Schmidt, J. M. Antineoplastic agents. 465, Structural modification of resveratrol: Sodium resverastatin phosphate. *J. Med. Chem.* **2002**, *45*, 2534−2542.
(62) Šmidrkal, J.; Harmatha, J.; Buděšínský, M.; Voráč, K.; Zídek, Z.; Kmoníčková, E.; Merkl, R.; Filip, V. Modified approach for preparing (*E*)-stilbenes related to resveratrol, and evaluation of their potential immunobiological effects. *Collect. Czech. Chem. Commun.* **2010**, *75*, 175−186.
(63) Han, S. Y.; Lee, H. S.; Choi, D. H.; Hwang, J. W.; Yang, D. M.; Jun, J.-G. Efficient total synthesis of piceatannol via (*E*)-selective Wittig-Horner reaction. *Synth. Commun.* **2009**, *39*, 1425−1432.
(64) Lee, H. S.; Lee, B. W.; Kim, M. R.; Jun, J.-G. Syntheses of resveratrol and its hydroxylated derivatives as radical scavenger and tyrosinase inhibitor. *Bull. Korean Chem. Soc.* **2010**, *31*, 971−975.
(65) Needs, P. W.; Kroon, P. A. Convenient syntheses of metabolically important quercetin glucuronides and sulfates. *Tetrahedron* **2006**, *62*, 6862−6868.
(66) Wang, L.-X.; Heredia, A.; Song, H.; Zhang, Z.; Yu, B.; Davis, C.; Redfield, R. Resveratrol glucuronides as the metabolites of resveratrol in humans: Characterization, synthesis, and anti-HIV activity. *J. Pharm. Sci.* **2004**, *93*, 2448−2457.
(67) Zhang, Z.; Yu, B.; Schmidt, R. R. Synthesis of mono- and di-*O*-β-D-glucopyranoside conjugates of (*E*)-resveratrol. *Synthesis* **2006**, *2006*, 1301−1306.
(68) Zhang, M.; Jagdmann, G. E., Jr.; Zandt, M. V.; Sheeler, R.; Beckett, P. Chemical synthesis and characterization of epicatechin glucuronides and sulfates: Bioanalytical standards for epicatechin metabolite identification. *J. Nat. Prod.* **2013**, *76*, 157−169.
(69) Radko, Y.; Christensen, K. B.; Christensen, L. P. Semi-preparative isolation of dihydroresveratrol-3-*O*-β-D-glucuronide and four resveratrol conjugates from human urine after oral intake of a

DOI: 10.1021/acsomega.9b00722
ACS Omega 2019, 4, 8222−8230

resveratrol-containing dietary supplement. *J. Chromatogr. B: Biomed. Sci. Appl.* **2013**, *930*, 54−61.
(70) Lucas, R.; Alcantara, D.; Morales, J. C. A concise synthesis of glucuronide metabolites of urolithin-B, resveratrol, and hydroxytyrosol. *Carbohydr. Res.* **2009**, *344*, 1340−1346.

DOI: 10.1021/acsomega.9b00722
ACS Omega 2019, 4, 8222−8230